Improving Parameter Extraction in Photovoltaic Models: The Role of Initialization Methods in Particle Swarm

Ismail Abazine[1*], Mustapha Elyaqouti[1], EL Hanafi arjdal[1], Driss Saadaoui[1], Imade Choulli[1] ,Dris Ben Hmamou[1] , Souad Lidaighbi[1] ,Abdelfattah Elhammoudy[1], Fatima Ezzahrae Souaidi[1], Ayoub Lahboub[1], and Brahim El fahmi[1]

[1]Laboratory of Materials, Signals, Systems and Physical Modelling, Faculty of Science, Ibn Zohr University, Agadir-Morocco

Abstract. This study investigates the effect of initialization strategies on the performance of Particle Swarm Optimization (PSO) for parameter extraction in photovoltaic (PV) models, specifically the Single Diode Model (SDM) and the Double Diode Model (DDM). Two initialization methods, Uniform Random Sampling Initialization (URSI) and Latin Hypercube Sampling (LHS), were compared to evaluate their impact on accuracy, stability, and computational efficiency. For the SDM, LHS reduced the mean RMSE from 1.7798×10^{-3} to 1.7127×10^{-3} (a 3.8% decrease) and the standard deviation by 19.7%, while maintaining a comparable computational time of 0.3988 s compared to 0.3948 s. In the DDM, LHS achieved a mean RMSE of 7.9489×10^{-4}, representing a 2.3% reduction relative to 8.1348×10^{-4}, and decreased the standard deviation by 50.4% from 1.2176×10^{-4} to 6.0390×10^{-5}, with nearly identical execution times. Overall, the results indicate that LHS significantly enhances the reliability and robustness of PSO by improving convergence stability and parameter accuracy under various operating conditions. These findings highlight the critical role of efficient initialization strategies in metaheuristic optimization for accurate and consistent PV system modelling.

Keywords: Photovoltaic Systems. Particle Swarm Optimization (PSO). Initialization. Single-Diode Model (SDM). Double Diode Model (DDM).

1 Introduction

In the field of renewable energy, particularly photovoltaic (PV) systems, substantial progress has been achieved in enhancing both efficiency and sustainability [1]. PV systems convert solar energy into electricity through solar cells and play a key role in the transition toward cleaner energy solutions [2]. Among the models used to analyze and optimize PV cell performance, the single-diode model (SDM) and double-diode model (DDM) are the most

* Corresponding author: abazine2@gmail.com

widely applied. The SDM offers a practical trade-off between simplicity and accuracy, whereas the DDM provides a more comprehensive representation of PV behavior under varying environmental conditions [3,4].

As shown in Fig. 1, the SDM represents a PV cell using a current source, a diode, and two resistors. The current source models the photocurrent, the diode simulates the P–N junction, and Rs and Rsh account for the internal and shunt resistances, respectively. These elements capture the electrical losses inherent in real PV systems.

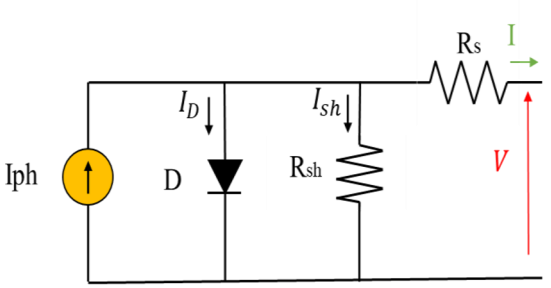

Fig. 1. The Single-Diode Model's (SDM) electrical circuit.

The relationship between current (I) and voltage (V) in the SDM is derived from Kirchhoff's laws and is given by the following equation:

$$\boldsymbol{I} = \mathrm{I_{ph}} - \mathrm{I_0}\left(\exp\left(\frac{\boldsymbol{V}+\mathrm{R_S}\boldsymbol{I}}{\mathrm{aV_t}}\right) - 1\right) - \frac{\boldsymbol{V}+\mathrm{R_S}\boldsymbol{I}}{\mathrm{R_{sh}}} \tag{1}$$

Here $\mathrm{I_0}$ is the dark saturation current; a is the diode ideality factor; $\mathrm{V_t}$ is the module thermal voltage and Iph is the photocurrent.

The DDM (see Fig. 2), an extension of the SDM, uses two diodes to more accurately represent a photovoltaic cell's performance, especially under low light conditions. One diode simulates the diffusion current, while the other accounts for charge recombination. The resistances Rs and Rsh still model internal losses and leakage currents.

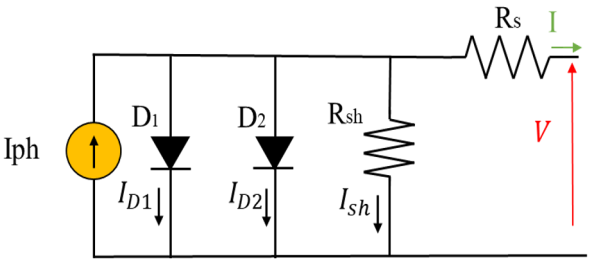

Fig. 2. The Double diode model (DDM) electrical circuit.

The mathematical model is provided by the relationship between the current (I) and the voltage (V), as governed by Kirchhoff's laws, in the expression below:

$$\boldsymbol{I} = \mathrm{I_{ph}} - \mathrm{I_{01}}\left(\exp\left(\frac{\boldsymbol{V}+\mathrm{R_S}\boldsymbol{I}}{\mathrm{a_1V_t}}\right) - 1\right) - \mathrm{I_{02}}\left(\exp\left(\frac{\boldsymbol{V}+\mathrm{R_S}\boldsymbol{I}}{\mathrm{a_2V_t}}\right) - 1\right) - \frac{\boldsymbol{V}+\mathrm{R_S}\boldsymbol{I}}{\mathrm{R_{sh}}} \tag{2}$$

In turn; I_{o1} and I_{o2} are the saturation and diffusion currents, correspondingly; and a_1 and a_2 are the ideality factors for recombination and diffusion, accordingly.

Determining the five unknown parameters in the Single Diode Model (SDM) or the seven unknown parameters in the Double Diode Model (DDM) is challenging due to their variability across different operating conditions. The methods in the literature are classified into three main categories: analytical techniques[5–7], numerical methods[8], and metaheuristic strategies[9,10].Metaheuristic methods, such as Particle Swarm Optimization (PSO) and Genetic Algorithms[15], stand out due to their ability to find global solutions in complex, non-linear problems. Unlike analytical and numerical approaches, which may struggle with accuracy or require good initial estimates, metaheuristic techniques excel in exploring large search spaces and solving multi-modal optimization problems. Despite their higher computational cost, these methods are powerful for achieving more reliable parameter estimation in a wide range of conditions.

Particle Swarm Optimization (PSO) [11]is particularly well suited for this type of problem. It is an optimization algorithm inspired by collective behaviors observed in nature, such as the coordinated movement of bird flocks or fish schools, which provides strong exploration and exploitation capabilities within the search space. Moreover, PSO is simple to implement and requires minimal parameter tuning, making it an accessible and efficient optimization technique for both researchers and practitioners.

Over the years, several variants of PSO have been proposed to enhance its performance and overcome the limitations of the standard version. Among these, Chaotic PSO [12](CPSO) and Fractional Order Darwinian PSO[13] (FODPSO) have shown improved balance between exploration and exploitation. CPSO introduces chaotic maps to increase population diversity and avoid premature convergence, while FODPSO integrates fractional-order dynamics inspired by Darwinian evolution to improve global search capability and convergence stability.

Beyond algorithmic improvements, the initialization phase of the swarm also plays a crucial role in determining both the convergence speed and the solution accuracy of PSO. In this study, two initialization strategies are investigated: Latin Hypercube Sampling[14] (LHS) and Uniform Random Sampling Initialization [15](URSI). LHS applies a stratified sampling technique to ensure a more uniform coverage of the search space, potentially leading to more consistent and robust results, whereas URSI provides a simpler yet efficient method for generating random initial positions.

The structure of this paper is as follows. Section 2 describes the methods, detailing the extraction of photovoltaic (PV) cell parameters using Particle Swarm Optimization (PSO), the formulation of the objective function, and the initialization strategies employed, namely Latin Hypercube Sampling (LHS) and Uniform Random Sampling Initialization (URSI). Section 3 presents and discusses the results, emphasizing the influence of the different initialization methods on the accuracy, stability, and computational efficiency of PSO, as well as environmental validation. Finally, Section 4 concludes the study and outlines potential directions for future research.

2 Methods and Materials

2.1 Extraction of PV cell parameters using Particle Swarm Optimization (PSO):

Particle Swarm Optimization (PSO) is a population-based metaheuristic inspired by collective behaviors observed in nature, such as bird flocking and fish schooling [11].

Originally proposed by Kennedy and Eberhart, PSO simulates a swarm of particles, each defined by a position x_i and velocity v_i, which evolve iteratively to optimize a given objective function. Particle movements are updated according to:

$$\mathbf{v_i^{(t+1)}} = \mathrm{w} * \mathbf{v_i^t} + \mathrm{c}_1 * \mathrm{r}_1 * (\mathbf{p_i} - \mathbf{x_i^t}) + \mathrm{c}_2 * \mathrm{r}_2 * \left(\mathbf{p_g} - \mathbf{x_i^t}\right) \quad (3)$$

$$\boldsymbol{x_i^{(t+1)}} = \boldsymbol{x_i^t} + \boldsymbol{v_i^{(t+1)}} \quad (4)$$

where w is the inertia weight, c_1 and c_2 are acceleration coefficients, r_1 and r_2 are random numbers uniformly distributed in [0,1], $\mathbf{p_i}$ is the personal best of particle i, and $\mathbf{p_g}$ is the global best position.

2.2 the objective function:

the Root Mean Square Error (RMSE) as the objective function, with the goal of estimating PV parameters by minimizing the error between estimated and experimental currents Experimental I–V data has been selected as objective functions. It is defined as below:

$$RMSE = \sqrt{\frac{\sum_i^N \left(I_{exp}(i) - I_{cal}(i)\right)^2}{N}} \quad (5)$$

In this context, Ical denotes the computed current value of the model, while Iexp denotes the measured current value. The variable N denotes the total count of observations considered.

To estimate the value of Ical, we use the Newton-Raphson method to solve Eq. (1) and (2), based on the combination of the estimated parameters.

2.3 initialization methods:

2.3.1 Latin hypercube sampling (LHS):

Latin Hypercube Sampling (LHS) improves the efficiency of sampling from multidimensional distributions by dividing each variable's range into N equal intervals and selecting one sample from each. This method offers better coverage compared to random sampling. The sampling process is governed by the equation:

$$x_{ij} = F^{-1}\left(\frac{r_{ij} + U[0,1]}{N}\right) \quad (6)$$

where X_{ij} represents the $j-th$ sample of the i-th variable, $F^{-1}$is the inverse cumulative distribution function (CDF), r_{ij} is a permutation of integers from 0 to N-1, and $U[0,1]$ is a uniform random variable. This approach ensures that each interval is represented in the sample, leading to more accurate results with fewer samples.

2.3.2 Uniform Random Sampling Initialization (URSI):

Uniform random sampling initialization is a method used to generate initial positions for particles (or other entities) within a defined range. This technique ensures that each position has an equal probability of being selected, which is crucial for effective exploration of the search space in optimization algorithms. The initialization process can be mathematically expressed as:

$$x_i = lb + (ub - lb) * U_i, \quad \forall i \in \{1, 2, \dots, n\} \tag{7}$$

Where $X_i$is the position of the i-th particle and U_i is a vector of dimension d whose elements u_j are independent samples uniformly distributed in the interval [0, 1]:

$$u_j \sim U(0, 1), \quad \forall j \in \{1, 2, \dots, d\} \tag{8}$$

3 Results and Discussion

3.1 Numerical results and discussion

The PSO algorithm parameters used are defined in Table 1.

Table 1. PSO parameters

Description	Parameters
Population size	20
Maximum iteration	250
C_1	1.5
C_2	1.5

The PSO algorithm was implemented in MATLAB R2024a and tested using the PV module described in Table 2, with upper and lower bounds for each parameter provided in **Table 3**. All simulations were conducted on a system equipped with an Intel Core i7 processor and 16 GB RAM running Windows 10, ensuring consistent computational performance.

Table 2. Electrical characteristics of RTC France PV modules at STC.

Electrical characteristic	R.T.C France
Imp: Current at MPP (A)	0.6894
Vmp: Voltage at MPP (V)	0.4507
Voc : Open-circuit voltage (V)	0.5728
Isc : Short-circuit current (A)	0.7603
Ns: Series-connected cells	1
G(W/m2)	1000
T(°C)	33

Table 3. Bounds of all parameters

	RTC France		ST40	
	Lb	***Ub***	***Lb***	***Ub***
a, a_1, a_2	1	2	1	2.5
I_0, I_{01}, I_{02} (μA)	0	1	0	100
$I_{\mathrm{ph}}(A)$	0	1	0	$2\times I_{SC}$
$R_{sh}(\Omega)$	0	100	0	5000
$R_S(\Omega)$	0	0.5	0	2

The best RMSE value (minimum) among 30 runs was selected for each algorithm to assess its accuracy.

Table 4 summarizes the key parameter values for the SDM, obtained using two classical PSO initializations (PSO_LHS and PSO_URSI) as well as the CPSO and FODPSO variants, including the corresponding RMSE value

Table 4. RMSE and parameter values for different PSO variants for the SDM.

	PSO_URSI	**PSO_LHS**	**FODPSO**[13]	**CPSO**[12]
RMSE(A)	8,0038E-04	8,0018E-04	9.7486E-04	9.6743E-04
a	1,450330	1,46391	1.4806	1.4706
$R_s(\Omega)$	0.0363779	0.036378	0.0364	0.0364
$R_{sh}(\Omega)$	46,39401	50,23810558	51.9512	50.9876
I_0(A)	2,36129E-07	2,71705E-07	3,187E-07	2,867E-07
I_{ph}(A)	0.7608765	0.7607465	0.7609	0.7608

Table 5 summarizes the key parameter values for the DDM, obtained using two classical PSO initializations (PSO_LHS and PSO_URSI) as well as the CPSO and FODPSO variants, including the corresponding RMSE values

Table 5. RMSE and parameter values for different PSO variants for the DDM.

	PSO_URSI	**PSO_LHS**	**FODPSO**	**CPSO**
RMSE(A)	7,4219E-04	7,4218E-04	9,6765E-04	9,6219E-04
a_1	1,9420	2	1,9768	2
a_2	1,4133	1,4368	1,3453	1,4567
Rs(Ω)	0,03735	0,03705	0,03776	0,03787
$R_{sh}(\Omega)$	55,8937	55,23696	55,342	55,26897
I_{01}(A)	1,15507E-06	9,73166E-07	9,76578E-07	9,565479E-07
I_{02}(A)	1,42321E-07	1,91646E-07	1,23453E-07	1,87941E-07
I_{ph}(A)	0.761	0.76079	0.75898	0.76067

The RMSE values for the SDM and DDM models are very similar across the PSO initialization methods (PSO_LHS and PSO_URSI), indicating that the choice of initialization has a negligible effect on the minimum RMSE obtained. In comparison, the more advanced PSO variants, namely CPSO and FODPSO, show slightly higher RMSE values, demonstrating that these additional mechanisms do not necessarily improve accuracy in this context. Overall, the PSO initialization methods provide robust and reliable performance for both models.

The convergence study for the SDM and DDM is presented in Fig. 3 and Fig. 4.

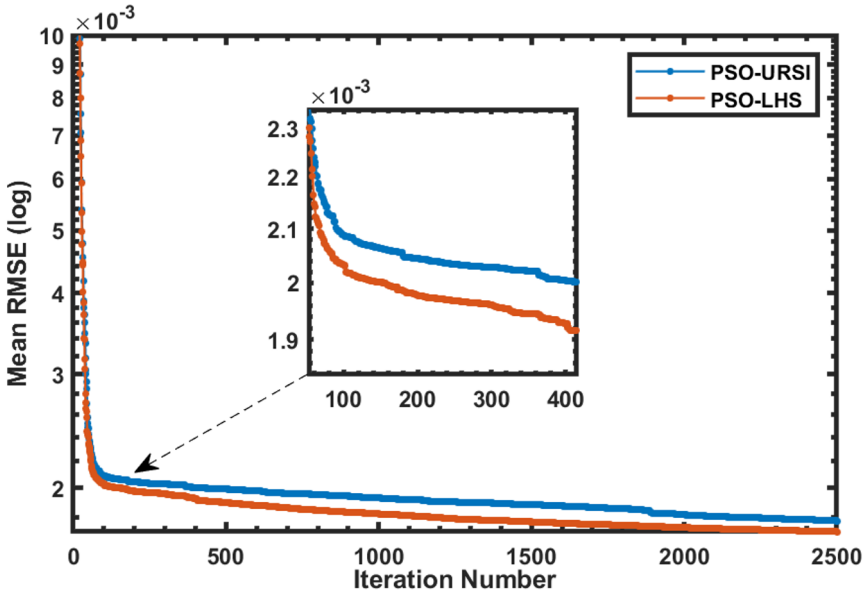

Fig. 3. Convergence Performance Evaluation of SDM

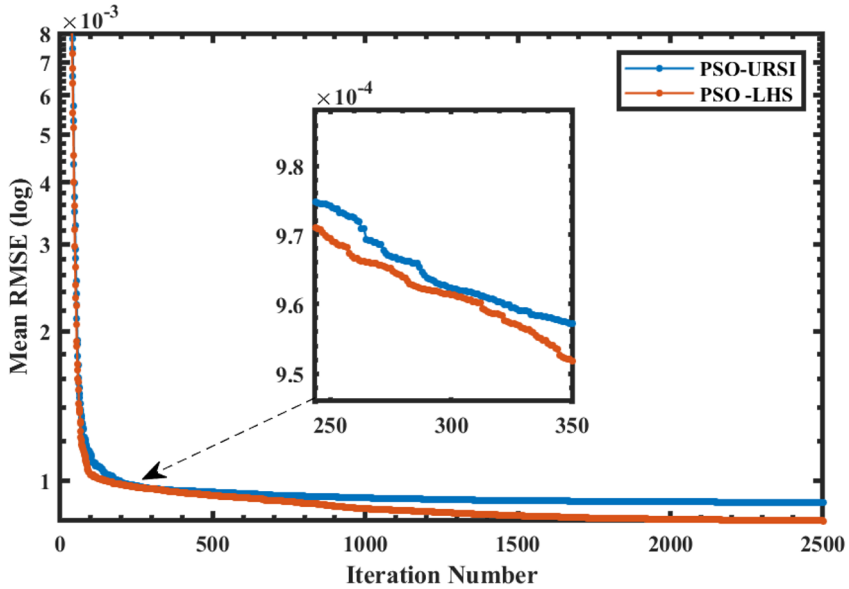

Fig. 4. Convergence Performance Evaluation of DDM.

Fig. 3 and Fig. 4 demonstrate that PSO-LHS and PSO-URSI exhibit nearly identical convergence patterns in the SDM and DDM models, although PSO-LHS shows a slight

displacement. Both methods converge towards a similar value after approximately 200 iterations. Consequently, PSO-LHS reveals particularly promising convergence characteristics.

The statistical results, including the mean (*mean*), maximum (*max*), minimum (*min*) values, and standard deviations (*Std*) of the objective functions (*RMSE*) for SDM and DDM, have been synthesized in Table 6.

Table 6. The outcomes from thirty tests conducted using both initialization methods with PSO.

		PSO_URSI	PSO_LHS
SDM	**Min**	8,0038E-04	8,0018E-04
	Max	2,0833E-03	2,0833E-03
	Mean	1,7798E-03	1,7127E-03
	Std	3,3151E-04	2,6635E-04
	time (s)	0.394755	0.39876
DDM	**Min**	7,4219E-04	7,4218E-04
	Max	1,4107E-03	9,6766E-04
	Mean	8,1348E-04	7,9489E-04
	Std	1,2176E-04	6,0390E-05
	time (s)	0.4678	0.4681

The results in Table 6 show that Latin Hypercube Sampling (LHS) significantly improves PSO performance compared to Uniform Random Sampling Initialization (URSI). For the SDM, the mean error decreases from 1.7798E-03 to 1.7127E-03 and the standard deviation from 3.3151E-04 to 2.6635E-04, while for the more complex DDM, the maximum error drops from 1.4107E-03 to 9.6766E-04, the mean error from 8.1348E-04 to 7.9489E-04, and the standard deviation from 1.2176E-04 to 6.0390E-05, with negligible impact on computational time.

These improvements are explained by the more uniform initial particle distribution provided by LHS, which ensures comprehensive exploration of the parameter space, reduces the risk of local minima, and enhances reproducibility. Overall, LHS stabilizes the optimization process and represents the most reliable initialization method for parameter extraction in both SDM and DDM models.

3.2 Validation of Results under Different Environmental Conditions

This subsection aims to evaluate the performance of the PSO_LHS algorithm in estimating the parameters of photovoltaic (PV) modules under varying environmental conditions. The short-circuit current $\mathrm{I}_{sc}(\mathrm{G},\mathrm{T})$ associated to non-standard conditions of temperature (T) and irradiance (G) is used to define the upper bound of the photogenerated current I_{ph} during the optimization process. The variation of $\mathrm{I}_{sc}(\mathrm{G},\mathrm{T})$ as a function of irradiance (G) and temperature (T) is described by the following equation:

$$I_{sc}(G,T) = I_{sc-STC} \cdot \frac{G}{G_{STC}} + k_i \cdot (\mathrm{T} - T_{STC}) \tag{9}$$

The parameters I_{sc-STC}, $T_{STC} = 25°C$ and $G_{STC} = 1000\, W.m^{-2}$ represent the short-circuit current, temperature, and irradiance under Standard Test Conditions (STC), respectively. The coefficient k_i corresponds to the temperature coefficient of the short-circuit current. All these values were extracted from the manufacturer's datasheets and are summarized in Table 7.

Table 7 Specifications of the tested PV module.

	ST40
k_i **(mA/°C)**	0.35
k_V **(mV/°C)**	-100
I_{sc-STC}**(A)**	2.68

The PSO_LHS algorithm was applied to extract the optimal parameters of the Thin Film ST40 photovoltaic module. The results presented in Table 8 summarize the estimated parameters under varying irradiance levels (at a constant temperature of 25 °C) and different temperatures (at a fixed irradiance of 1000 W/m²).

Table 8 Estimated parameters of the Thin Film ST40 PV module obtained by the PSO_LHS algorithm under multiple irradiance and temperature conditions.

	Parameters	**Irradiance**				
ST 40	$G(W/m^2)$	***200***	***400***	***600***	***800***	***1000***
	$I_{ph}(A)$	0.54039418	1.077436189	1.60675625	2.1383866	2.70735781
	$I_0(A)$	0.0001000	2.60761E-05	1.8932E-05	7.8288E-06	2.5663E-08
	$R_s(\Omega)$	1.0612653	0.65300056	0.8127182	0.7798617	1.2437391
	$R_{sh}(\Omega)$	582.08604	711.3432418	1341.3059	1736.9482	217.54073
	a	2.2047323	2.222265261	2.2141325	2.2168971	1.5062528
	RMSE(A)	**3.7697E-03**	**4.08677E-03**	**7.2645E-03**	**1.1369E-02**	**1.221E-02**
	R^2	**0.9997**	**0.9996**	**0.9989**	**0.9973**	**0.9969**
	Parameters	**Temperatures**				
	$T(°C)$	*20*	*40*	*60*		
	$I_{ph}(A)$	2.67763651	2.7172291457	2.76051158		
	$I_0(A)$	7.28247E-06	1.22889E-05	4.4586E-05		
	$R_s(\Omega)$	0.90582638	1.047027741	1.13048445		
	$R_{sh}(\Omega)$	700.383654	317.519569	254.241739		
	a	2.04058494	1.82841972	1.74662564		
	RMSE(A)	**1.4441E-02**	**1.59996E-02**	**2.1061E-02**		
	R^2	**0.9963**	**0.9958**	**0.9941**		

The analysis of the obtained results highlights the robustness and precision of the proposed approach. The RMSE values, ranging from 10^{-3} to 10^{-2}, demonstrate the strong predictive capability and numerical stability of the model. Moreover, the R^2 coefficients, which lie between 0.9969 and 0.9997, confirm the excellent agreement between the simulated and experimental I–V characteristics.

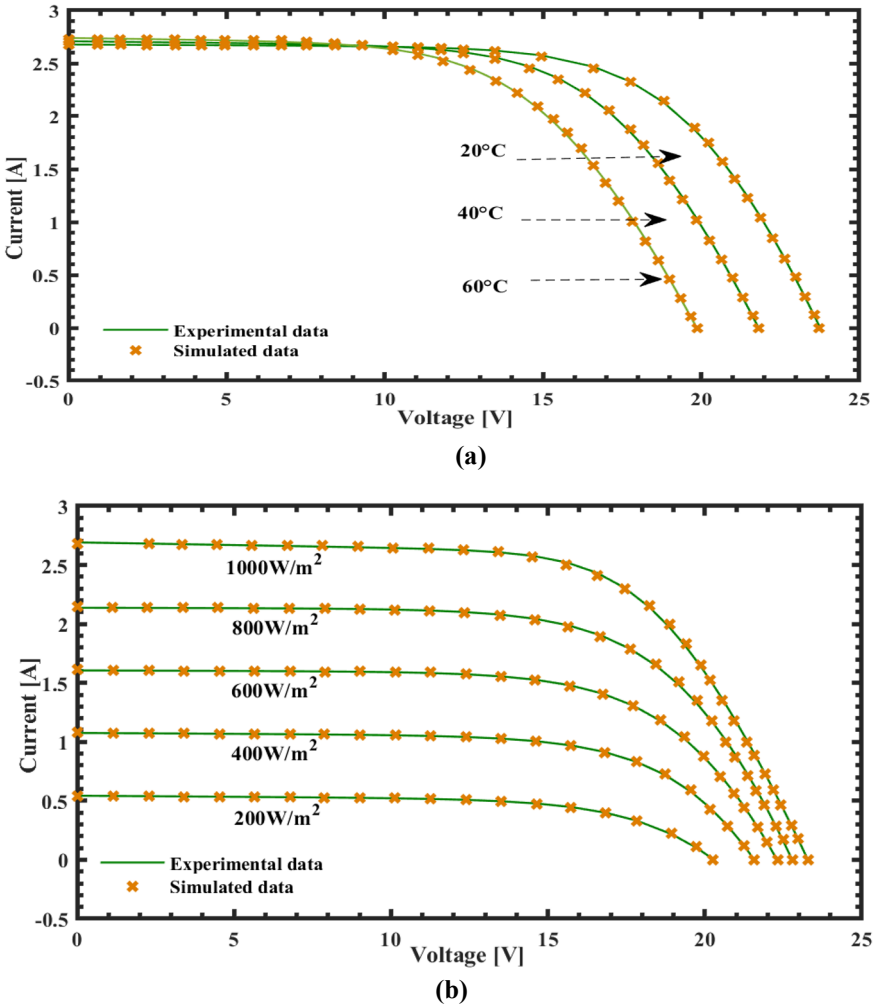

Fig. 5. Comparison of experimental and simulated data for the Thin Film ST40 module: (a) at different temperatures, (b) under varying irradiance.

To visually support these findings, Fig. 5 depicts the I–V curves of the Thin Film ST40 module under various irradiance and temperature conditions, clearly showing the strong correspondence between experimental and simulated data.

In addition, Fig. 6 illustrates the absolute current error (IAE) distributions, further emphasizing the low deviation and high accuracy of the proposed PSO_LHS. These results validate the effectiveness and reliability of the algorithm in accurately determining PV model parameters across diverse environmental scenarios.

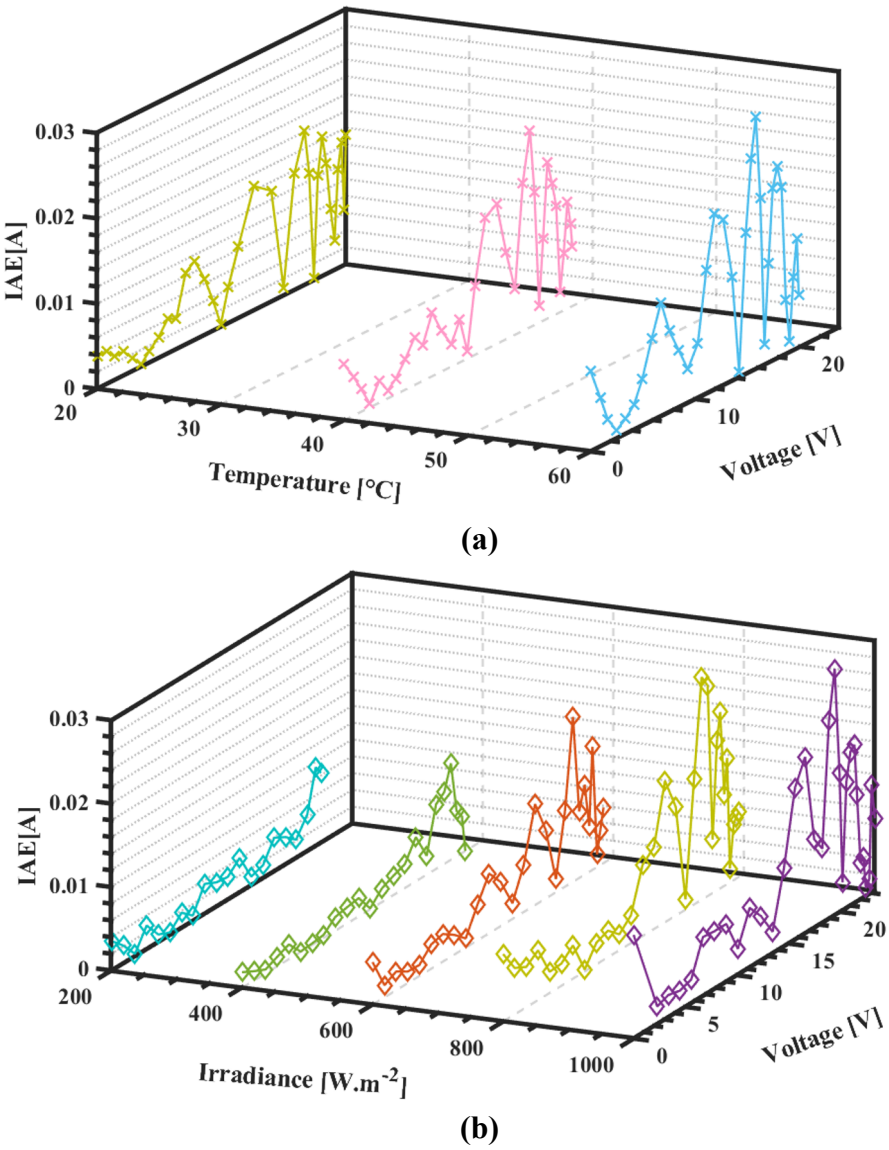

Fig. 6. Current absolute error curves for ST 40 Thin film (a) different temperature and at 1000W/m^2 (b) different irradiation and at 25°C.

4 Conclusion

In conclusion, this study demonstrates that Latin Hypercube Sampling (LHS) significantly improves the performance of Particle Swarm Optimization (PSO) for parameter extraction in the Single Diode Model (SDM) and Double Diode Model (DDM) of photovoltaic systems. LHS produces lower mean errors and reduced standard deviations compared to Uniform

Random Sampling Initialization (URSI), highlighting its reliability and robustness. The choice of initialization method is crucial in metaheuristic optimization, as proper initialization enhances convergence speed and solution quality. Moreover, the results show that LHS maintains its effectiveness under varying environmental conditions, demonstrating consistent performance across different operating scenarios. This research emphasizes the importance of effective initialization strategies, paving the way for more efficient and resilient modeling techniques in renewable energy systems

References

1. R. TAMRAKAR and A. GUPTA, IJIREEICE (2015)
2. M. Ćalasan, S. H. E. Abdel Aleem, and A. F. Zobaa, Energy Convers. Manag. **210**, 112716 (2020)
3. I. Abazine, M. Elyaqouti, E. H. Arjdal, D. Saadaoui, D. Ben Hmamou, A. Elhammoudy, S. Lidaighbi, and I. Choulli, E-Prime - Adv. Electr. Eng. Electron. Energy **11**, 100935 (2025)
4. A. Asbayou, A. Aamoume, M. Elyaqouti, A. Ihlal, and L. Bouhouch, Int. J. Electr. Comput. Eng. **12**, 102 (2022)
5. M. Calasan, S. Vujosevic, M. Micev, M. Alruwaili, and A. A. Wijaya, Alexandria Eng. J. **104**, 95 (2024)
6. H. El Achouby, M. Zaimi, A. Ibral, and E. M. Assaid, Energy Convers. Manag. **177**, 258 (2018)
7. J. C. H. Phang, D. S. H. Chan, and J. R. Phillips, Electron. Lett. **20**, 406 (1984)
8. I. Choulli, D. Ben hmamou, E. hanafi Arjdal, D. Saadaoui, S. Lidaighbi, A. Elhammoudy, S. Obukhov, and A. Ibrahim, Energy Convers. Manag. X **18**, (2023)
9. K. Ishaque, Z. Salam, S. Mekhilef, and A. Shamsudin, Appl. Energy **99**, (2012)
10. I. Abazine, M. Elyaqouti, E. H. Arjdal, D. Saadaoui, D. Ben Hmamou, A. Elhammoudy, S. Lidaighbi, I. Choulli, and B. Ydir, Int. J. Hydrogen Energy **139**, 564 (2025)
11. T. S. Babu, J. P. Ram, T. Dragičević, M. Miyatake, F. Blaabjerg, and N. Rajasekar, IEEE Trans. Sustain. Energy **9**, (2018)
12. W.-C. Hong, Energy Convers. Manag. **50**, 105 (2009)
13. W. A. E. M. Ahmed, H. M. A. Mageed, S. A. Mohamed, and A. A. Saleh, Alexandria Eng. J. **61**, 1249 (2022)
14. J. O. Agushaka and A. E. Ezugwu, Appl. Sci. **12**, 896 (2022)
15. Q. Li, Y. Bai, and W. Gao, IEEE Access **9**, 121366 (2021)